JOURNAL OF VIROLOGY, Oct. 1994, p. 6291–6298
0022-538X/94/$04.00+0

Vol. 68, No. 10

Semliki Forest Virus Infects Mouse Brain Endothelial Cells and Causes Blood-Brain Barrier Damage

MERJA SOILU-HÄNNINEN,[1]* JUHA-PEKKA ERÄLINNA,[1] VEIJO HUKKANEN,[1,2] MATIAS RÖYTTÄ,[3] AIMO A. SALMI,[1] AND REIJO SALONEN[1,4]

Departments of Virology,[1] Pathology,[3] and Neurology[4] and the MediCity Research Center,[2] University of Turku, Turku, Finland

Received 17 February 1994/Accepted 17 June 1994

Induction of experimental allergic encephalomyelitis is facilitated in a genetically resistant BALB/c mouse strain by a nonpathogenic strain of a neurotropic alphavirus, Semliki Forest virus (SFV-A7). One possible explanation for this enhancement is virus infection of endothelial cells (EC), causing increased permeability of the blood-brain barrier. We have now sought evidence for virus infection of EC in vivo by immunocytochemistry and in situ hybridization. SFV-A7 antigens and RNA were detected in vascular EC and perivascular neurons in cerebellar and spinal cord white matter. Expression of viral antigens was followed by fibrinogen leakage from the blood vessels into brain parenchyma. This was shown by immunoperoxidase staining detecting fibrinogen extravascularly in central nervous system sections of infected mice. Simultaneously, expression of ICAM-1 (intercellular adhesion molecule 1) was induced on brain EC. SFV-A7 replicated in mouse brain microvascular EC in vitro and caused lysis of the cells. SFV-A7 did not induce ICAM-1 expression of mouse brain microvascular EC in vitro, while ICAM-1 was readily induced by gamma interferon and interleukin 1β. The observed increase of ICAM-1 expression on EC is immune mediated and not a direct effect of the virus infection. We conclude that SFV-A7 infection causes cerebral microvascular damage which contributes to the facilitation of experimental allergic encephalomyelitis in BALB/c mice.

Relapse phases of multiple sclerosis (MS) are associated with viral infections (3, 37), but it is not known how virus infections modulate this autoimmune demyelinating disease. Blood-brain barrier (BBB) damage caused by virus infection is one possible mechanism, since increased BBB permeability is an early and possibly crucial event in the pathogenesis of new lesions in MS (22) and some viral infections are also known to cause vascular permeability changes. Vascular injury is a central feature of some hemorrhagic fevers (10, 35), and BBB damage has been shown during human immunodeficiency virus encephalitis (29) and uncomplicated measles virus infection (19).

It is largely unknown whether the increased vascular permeability during virus infection is caused by virus replication in endothelial cells (EC), virus-induced cytokines, anti-EC antibodies raised during the virus infection, or other yet unknown mechanisms (41). Several common viruses such as herpes simplex, mumps, and measles viruses and many enteroviruses are able to infect cultured EC derived from either human umbilical vein or dermal microvessels (1, 14). Although susceptibility in vitro does not confer susceptibility in vivo, many of these viruses have been shown to infect human or animal EC also in vivo (5, 18, 42, 43). Whether infection of EC by these common viruses in vivo leads to increased vascular permeability is not well known.

Experimental allergic encephalomyelitis (EAE) is an animal model in which a clinically and histologically MS-like disease is induced in susceptible strains of laboratory animals by active immunization with neuroantigen in complete Freund's adjuvant or by transfer of T cells specific for brain antigens (26). We have earlier described an EAE model in which the disease is facilitated in a genetically resistant mouse strain, BALB/c, by infection with an avirulent mutant of a neurotropic alphavirus, Semliki Forest virus (SFV-A7) (7), 7 days after the induction of EAE (44). However, the mechanisms by which the virus facilitates EAE in BALB/c mice have not been established.

Adhesion molecules have been shown to have a central role in recruitment of leukocytes into the central nervous system (CNS) during inflammation. Induction of intercellular adhesion molecule 1 (ICAM-1) in inflammation is an important means of regulating leukocyte-EC interactions (39). Increased influx of inflammatory cells into the CNS correlates with upregulation of ICAM-1 in mouse EAE (9), and initiation of BBB damage in MS correlates with increased levels of circulating ICAM-1 in the serum and in the cerebrospinal fluid of MS patients (36). Increased cytokine-induced expression of ICAM-1 on cultured murine cerebrovascular EC results in increased adhesion of myelin basic protein-specific encephalitogenic T cells to the EC (25). In addition, antibodies to ICAM-1 have been shown to inhibit EAE in Lewis rats (4). Virus infection may also have an effect on the expression of adhesion molecules. Induction of ICAM-1 has been described during herpes simplex virus encephalitis in humans (38), and increased expression of vascular cell adhesion molecule 1 on brain vessels has been shown in macaque simian immunodeficiency virus encephalitis (34).

In this report, we extend our earlier studies of facilitation of BALB/c mouse EAE by SFV-A7. Since virus infection of EC leading to BBB damage is one possible explanation for the enhancement, we have sought evidence for viral invasion of cerebral EC by immunohistochemical staining and by hybridization in situ. To study the function of the BBB, we have done immunostaining for serum protein fibrinogen in mouse brain. Facilitation of leukocyte entry into the CNS by induction of adhesion molecules is another possible mechanism of enhancement of CNS autoimmunity. Therefore, we have studied the expression of ICAM-1 during SFV-A7 infection. The results

* Corresponding author. Mailing address: University of Turku, Department of Virology, Kiinamyllynkatu 13, 20520 Turku, Finland. Phone: 358-21-6337461. Fax: 358-21-2513303.

indicate that SFV-A7 infects cerebral EC, leading to BBB damage and induction of ICAM-1 expression in mouse brain. To study in more detail how SFV-A7 infection induces ICAM-1 expression and causes increased vascular permeability, we have established a system for culturing mouse brain microvascular EC (MBMEC). We show that SFV-A7 infects MBMEC, leading to lysis of the cells, but it does not induce ICAM-1 in vitro.

MATERIALS AND METHODS

Mice. BALB/c mice were raised at the Central Animal Laboratory of the University of Turku from breeder stocks obtained from Harlan Sprague-Dawley, Inc., Indianapolis, Ind. Female mice at age 6 to 8 weeks were used for experiments in vivo. The MBMEC cultures were from 3- to 4-day old mouse pups.

Virus. An avirulent strain of SFV (SFV-A7) was obtained from H. E. Webb (Neurology Unit, Department of Neurology, Rayne Institute, St. Thomas's Hospital, London, United Kingdom) and grown in a BALB/c mouse brain cell line (MBA-1) previously established in this laboratory. The virus was titrated in another BALB/c brain cell line (MBA-13) by a standard plaque assay technique. The virus was stored in 1-ml aliquots at −70°C.

Antibodies, cytokines, and cell culture reagents. Fluorescein isothiocyanate (FITC)-labeled *Griffonia simplicifolia* isolectin-B4 (GSA-FITC) was from Sigma Chemicals (St. Louis, Mo.). Dioctadecyltetramethylindocarbocyanine perchlorate-labeled acetylated low-density lipoprotein (DiI-Ac-LDL) was obtained from Biomedical Technologies Inc. (Stoughton, Mass.). Rabbit anti-human glial fibrillary acidic protein was from Zymed (San Francisco, Calif.), and FITC-conjugated porcine anti-rabbit immunoglobulin G (IgG) was from Wellcome (Dartford, United Kingdom). Mouse and rabbit polyclonal antibodies to SFV-A7 were raised by immunization with inactivated SFV-A7 virus. Rabbit antibodies against human factor VIII (FVIII) and lissamine rhodamine-conjugated goat anti-rabbit IgG were from Accurate (Westbury, N.Y.), and FITC-conjugated goat anti-mouse IgG was from Zymed. Rat hybridoma cell clone CRL 1878 (Y.N./1.7.4.) producing monoclonal antibody reactive with murine ICAM-1 was from the American Type Culture Collection (Rockville, Md.), rabbit anti-human fibrinogen antibody was from Dako (Glostrup, Denmark), and Vectastain peroxidase anti-rat (PK-4004) and anti-rabbit (PK-4001) antibody kits were from Vector Laboratories Inc. (Burlingame, Calif.). Diaminobentzidintetrahydrochloride (DAB) was from Sigma Chemicals. Recombinant murine gamma interferon and interleukin-1β were purchased from Genzyme (Boston, Mass.). EC growth supplement, cyclic AMP (cAMP), and gelatin were from Sigma. Heparin was from Leiras (Turku, Finland), and Percoll was from Pharmacia (Uppsala, Sweden). Culture plates were from Costar (Cambridge, Mass.) and Nunc (Roskilde, Denmark).

SFV-A7 infection of mice. Female BALB/c mice at age 6 to 8 weeks were infected intraperitoneally by 10^6 PFU of SFV-A7 in a 100-μl volume of sterile phosphate-buffered saline (PBS). No signs of clinical illness developed during a 3-week observation period. On days 1 to 8 and on day 20, a group of four mice were perfused with PBS under anesthesia. The brains and spinal cords were then removed, cut into thin sections, and rapidly frozen in Tissue-Tek (Miles Inc., Naperville, Ill.) by immersion in liquid nitrogen. The blocks were stored at −70°C until use. In addition, two animals under anesthesia were sacrificed daily from day 0 to day 7 and perfused with formalin for preparation of paraffin-embedded brain and spinal cord specimens.

Immunohistochemistry. Immunoperoxidase staining for fibrinogen and SFV-A7 antigens was done on parallel deparaffinized cerebellar and spinal cord sections of infected mice with rabbit antibody to fibrinogen and rabbit antibody to SFV-A7. Binding of primary antibodies was demonstrated by avidin-biotin complex technique with Vectastain anti-rabbit antibody kit according to the manufacturer's instructions. The color reaction was developed with DAB as chromogen. The sections were counterstained with Mayer's hematoxylin.

For double-immunofluorescence labeling, 6-μm frozen CNS sections of SFV-A7-infected and control mice were cut on a cryotome, air dried, and fixed in cold acetone for 10 min. The sections were first incubated with rabbit antibodies to human FVIII and mouse polyclonal anti-SFV-A7 antiserum (diluted in PBS to 1:100 and 1:200, respectively) for 60 min at +37°C in a humid chamber, washed three times for 5 min each with PBS, and further incubated with lissamine-rhodamine-conjugated goat anti-rabbit IgG and FITC-conjugated goat anti-mouse IgG for 30 min at +25°C. After washes, the samples were air dried and mounted in Vectashield (Vector Laboratories Inc.). Confocal microscopy analysis was performed with a beam-scanning confocal fluorescent microscope (European Molecular Biology Laboratory compact confocal microscope with Zeiss Axiovert/10 microscope and 100×-1.3 oil Plan-Neofluor objective) with laser excitation at 488 nm for FITC and 514 nm for lissamine-rhodamine. Some of the slides were viewed under rhodamine and fluorescein filters of a Leitz Dialux 22 inverted fluorescence microscope.

For detection of ICAM-1, 6-μm frozen sections from infected and control mice were stained with diluted Y.N./1.7.4. hybridoma supernatant reactive with murine ICAM-1. The Vectastain anti-rat antibody staining kit was used to demonstrate binding of the primary antibody.

In situ hybridization. The SFV-A7 probe was from the E1 region of the viral genome, corresponding to the nucleotides 10658 to 10953 of the wild-type virus cDNA. The probe DNA was released by digestion with *Eco*RI from a clone, prepared by PCR from SFV-A7 cDNA, and purified from the vector (pCRII; In vitrogen) by electrophoresis through an agarose gel. The DNA was eluted from agarose by use of agarase enzyme (Boehringer Mannheim). The fragment was labeled with digoxigenin (DIG)-11-dUTP by random priming with the DIG DNA labeling and detection kit (Boehringer Mannheim), as described previously (21).

Sections of formalin-fixed, paraffin-embedded mouse CNS tissue were cut at a 5-μm thickness and mounted on organosiliconized slides (24). Sections from uninfected mice as well as MBA-13 cells, uninfected or infected with SFV-A7 (10 PFU per cell) and harvested at 8 h postinfection, were used as hybridization controls. The in situ hybridization was done as described previously for DIG DNA probes (21), and it involved a prehybridization step using 300 μg of denatured salmon sperm DNA per ml and the use of mouse brain nucleic acids (500 μg/ml) as a blocking agent in the hybridization buffer. The hybridization took place for 21 h at +42°C under sealed caps in a humidified incubator. The slides were washed as described in reference 33 and subjected to the nonradioactive detection protocol (21). Briefly, the sections were incubated in 1% blocking reagent of the DIG DNA labeling and detection kit for 30 min at +20°C, incubated with the alkaline phosphatase-conjugated anti-DIG antibody (750 mU/ml) in a humid chamber for 30 min at +20°C, and washed and incubated with the nitroblue tetrazolium–X-phosphate color reagents in a dark, humidified chamber for 8 to 16 h. The slides

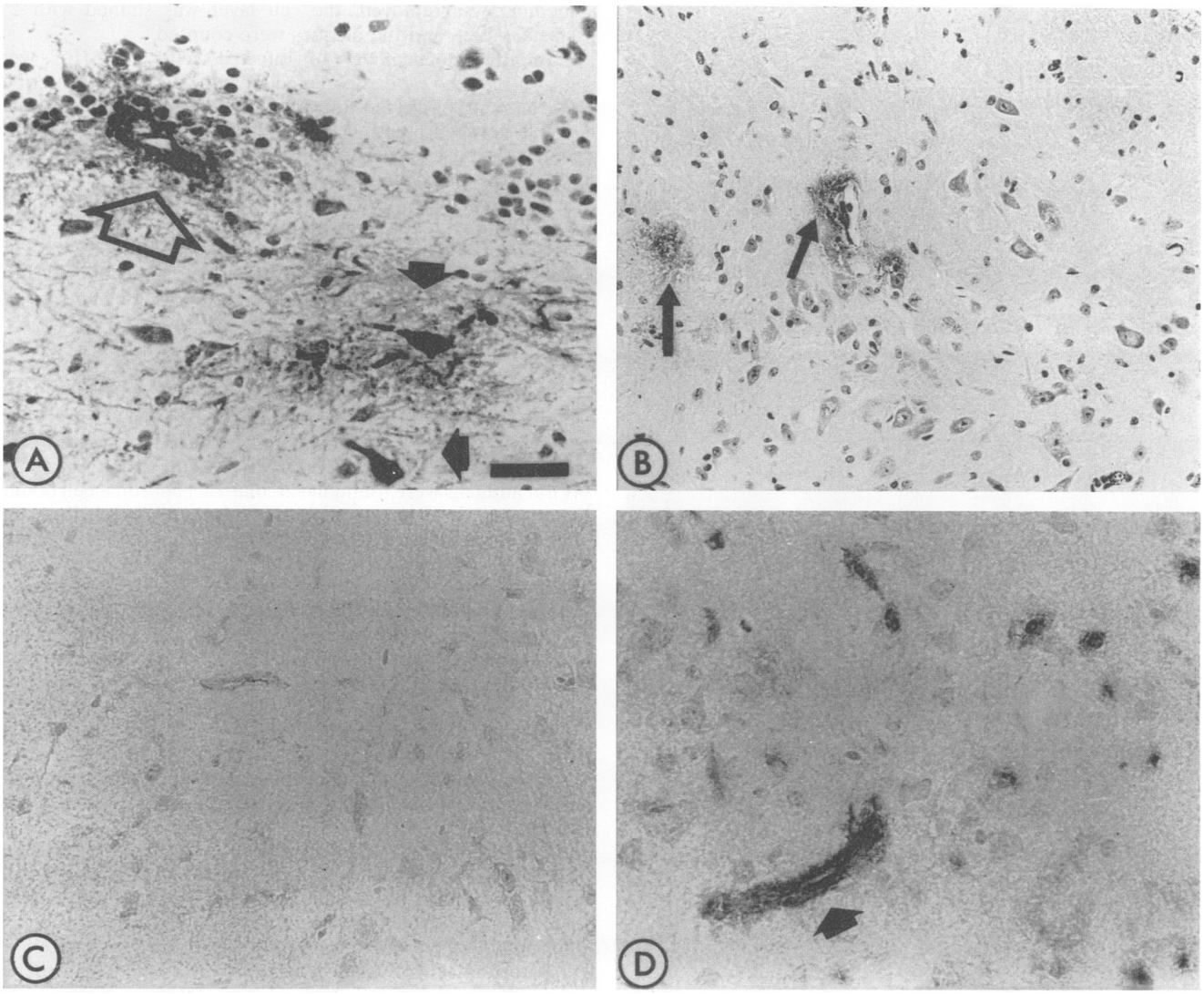

FIG. 1. Detection of SFV-A7 antigens, fibrinogen, and ICAM-1 in mouse brain. Panel A shows expression of SFV-A7 antigens, and panel B shows detection of fibrinogen in a pons area of BALB/c mouse brain 5 days p.i. with 10^6 PFU of the virus. The mice were anesthetized and perfused with formalin. Paraffin-embedded brain sections were stained with rabbit polyclonal antibody to SFV-A7 (A) and rabbit antibody to human fibrinogen (B) by avidin-biotin complex technique. In panel A, an immunoreactive vessel is indicated with an arrow. The closed arrow indicates infected perivascular neurons. In panel B, arrows indicate detection of fibrinogen in extravascular space. Panels C and D show ICAM-1 expression in pons area of BALB/c mouse brain. Immunoperoxidase staining with monoclonal antibody Y.N./1.7.4. reactive with murine ICAM-1 was done from 6-μm frozen CNS sections. Panel C represents normal mouse brain, and panel D represents infected brain 5 days p.i. The arrow in panel D indicates the blood vessel wall. All sections have been counterstained with hematoxylin. Magnification: the scale bar shown in panel A represents 23 μm for panels A and D, 28 μm for panel B, and 30 μm for panel C.

were stained slightly with hematoxylin-eosin or eosin only, and the coverslips were mounted with Gurr's Aquamount. The slides were observed in a blinded fashion.

Culture of MBMEC. MBMEC were isolated and cultured according to the method described by L. de Bault et al. (11) with some modifications. Briefly, 10 BALB/c mouse pups were killed by cervical dislocation, and their brains were aseptically removed, washed in isolation medium (Dulbecco modified Eagle medium, 25 mM HEPES [*N*-2-hydroxyethylpiperazine-*N'*-2-ethanesulfonic acid], 100 IU of penicillin per ml, 100 μg of streptomycin per ml, and 1 μg of amphotericin B [Fungizone] per ml = medium A), mechanically homogenized, and sequentially filtered through 145- and 55-μm nylon screens. The material retained on 55-μm screens was spun for 10 min at 1,000 × *g* on 50% Percoll gradients prepared as described by Goldstein et al. (16). The upper band containing microvessel fragments was removed with a Pasteur pipette, washed twice in medium A, resuspended in growth medium (medium A containing 2 mM glutamine, 20% fetal calf serum, 75 μg of EC growth supplement per ml, 40 μg of heparin per ml, and 240 μg of cAMP per ml), and plated onto gelatin-coated 50-cm^2 Nunclon tissue culture flasks. Culture medium was changed every 2 to 3 days. The EC were grown into confluence and passaged for identification and experiments with trypsin-EDTA. The cells were identified as EC by staining the cells grown on glass coverslips with 100 μg of GSA-FITC per ml for 1 h at 37°C (32) and by assessing incorporation of DiI-Ac-LDL diluted to 10 μg/ml in growth medium during a 4-h incubation

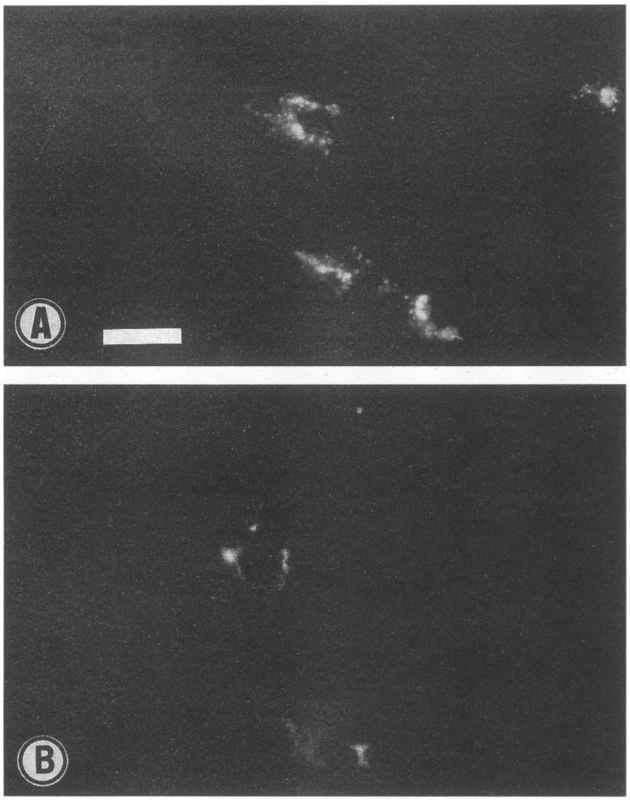

FIG. 2. Double immunolabeling of BALB/c mouse CNS sections for FVIII and SFV-A7 antigens. Panel a shows FVIII labeling, and panel b shows staining for virus antigens. The mice were infected intraperitoneally with 10^6 PFU of SFV-A7, and the whole body was perfused with PBS via left cardiac chamber under anesthesia at day 4 p.i. Frozen sections were prepared, and double immunofluorescence staining with rabbit anti-human FVIII antibodies and mouse anti-SFV-A7 antiserum was done as described in Materials and Methods. Magnification: scale bar = 20 μm.

on live cells (40). Astrocyte contamination was examined by staining with rabbit anti-human glial fibrillary acidic protein followed by FITC-conjugated porcine anti-rabbit IgG. The cells were stained for flow cytometry with 20 μg of GSA-FITC per ml and analyzed with FACScan (Becton Dickinson, San Jose, Calif.).

Infection of MBMEC with SFV-A7. The MBMEC at the second or third passage were grown into confluence on round 18-mm coverslips placed in 12-well tissue culture plates. The cell monolayers were washed twice with warm PBS and inoculated with SFV-A7 (multiplicity of infection [MOI] of 10). The virus was allowed to adhere on cell monolayers for 1 h at 37°C in a CO_2 incubator, the cultures were washed twice with Dulbecco modified Eagle medium, and 2 ml of growth medium was added to each well. Samples for plaque titration were taken from culture supernatant at 0, 5, 10, 22, 29, 47, and 71 h after medium replacement and stored at −70°C until titrated.

Plaque titration. Serial 10-fold dilutions of the collected, cell-free supernatants were inoculated in duplicate 100-μl volumes onto MBA-13 cells grown in 12-well tissue culture plates. After the virus was allowed to adhere for 1 h, medium containing three parts of 2% modified Eagle medium and one part of 4% carboxymethyl cellulose and 2× Hanks salt solution was gently added to the wells. After 48 h of incubation, the medium was removed, the cell layer was stained with 2% crystal violet, and the plaques were counted.

Immunocytochemistry of infected cells. MBMEC were grown on glass coverslips, infected with SFV-A7 as described above, and harvested for immunofluorescence at six time points between 6 and 72 h postinfection (p.i.). The coverslips were washed with PBS, fixed in cold acetone, and incubated with rabbit polyclonal antiserum to SFV-A7 for 1 h at 24°C in a moist chamber; washed three times with PBS; and incubated for 30 min with goat antiserum to rabbit IgG conjugated with lissamine-rhodamine. After a further washing cycle, the cells were incubated with GSA-FITC for 1 h, washed, air dried, and mounted in Fluoromount (BDH Ltd., Poole, England).

RESULTS

Detection of SFV-A7 antigens in vivo. To reveal whether mouse brain EC are infected after intraperitoneal infection of mice with SFV-A7, brain sections of infected and control mice were stained for SFV antigens with specific rabbit antiserum. Viral antigens were found in vascular EC, neuronal cell bodies, axons, and dendrites of cerebral hemispheres, cerebellum, and spinal cord. The virus antigens first appeared on day 2, peaked on day 4, and disappeared after day 7 p.i. (Fig. 1A). The lesions were focally distributed throughout the CNS and concentrated around small blood vessels. Positive staining appeared first and was most abundant in cerebellar and pons white matter. Control mice were negative.

To differentiate EC from astrocytes, perivascular microglia, or pericytes, double labeling with rabbit anti-human FVIII antibodies and mouse SFV-A7-specific antiserum was done on frozen CNS sections. Light microscopy (Fig. 2B) and confocal microscopy (not shown) showed expression of viral antigens in cells identified as EC with the typical granular pattern of FVIII staining (Fig. 2A).

BBB damage closely correlating with the regional and chronological distribution of the spread of the virus in the brain was shown by detecting fibrinogen in the brain parenchyma of infected mice (Fig. 1B). In uninfected mice, no fibrinogen was found outside the blood vessels.

Detection of viral RNA by in situ hybridization. In order to characterize the distribution of viral RNA in tissues, CNS sections of infected and control mice were hybridized in situ with a nonradioactive probe from the E1 region of the viral genome. An average total of 29 CNS tissue sections from two mice were examined for each time point of infection. Three uninfected mice were included as hybridization controls. SFV-A7 RNA was observed in capillary EC and in neuronal cell bodies in cerebellum, midbrain, spinal cord, and cerebral hemispheres (Fig. 3). Cells reactive with the A7 probe were first detected on day 1 after the virus inoculation (Table 1). The number of cells reactive with the probe was highest on days 3 to 4 p.i., decreasing to less than one positive cell per section by day 7 p.i. The cells positive for A7 RNA appeared typically in foci surrounding small blood vessels in the CNS. The SFV-A7 RNA-positive EC were observed on days 1 to 4 p.i. The MBA-13 cells, infected in culture with SFV-A7, were strongly positive for the probe at 8 h p.i.

ICAM-1 expression in vivo. To study whether expression of an inducible adhesion receptor, ICAM-1, is enhanced during the course of CNS inflammation caused by SFV-A7 infection, immunoperoxidase staining for ICAM-1 on SFV-A7-infected and control brains was done. In brain tissue of normal, 6- to 8-week-old female BALB/c mice, expression of ICAM-1 was low with a faint staining only on a few vessels (Fig. 1C). During SFV-A7 infection, the number of ICAM-1-positive microves-

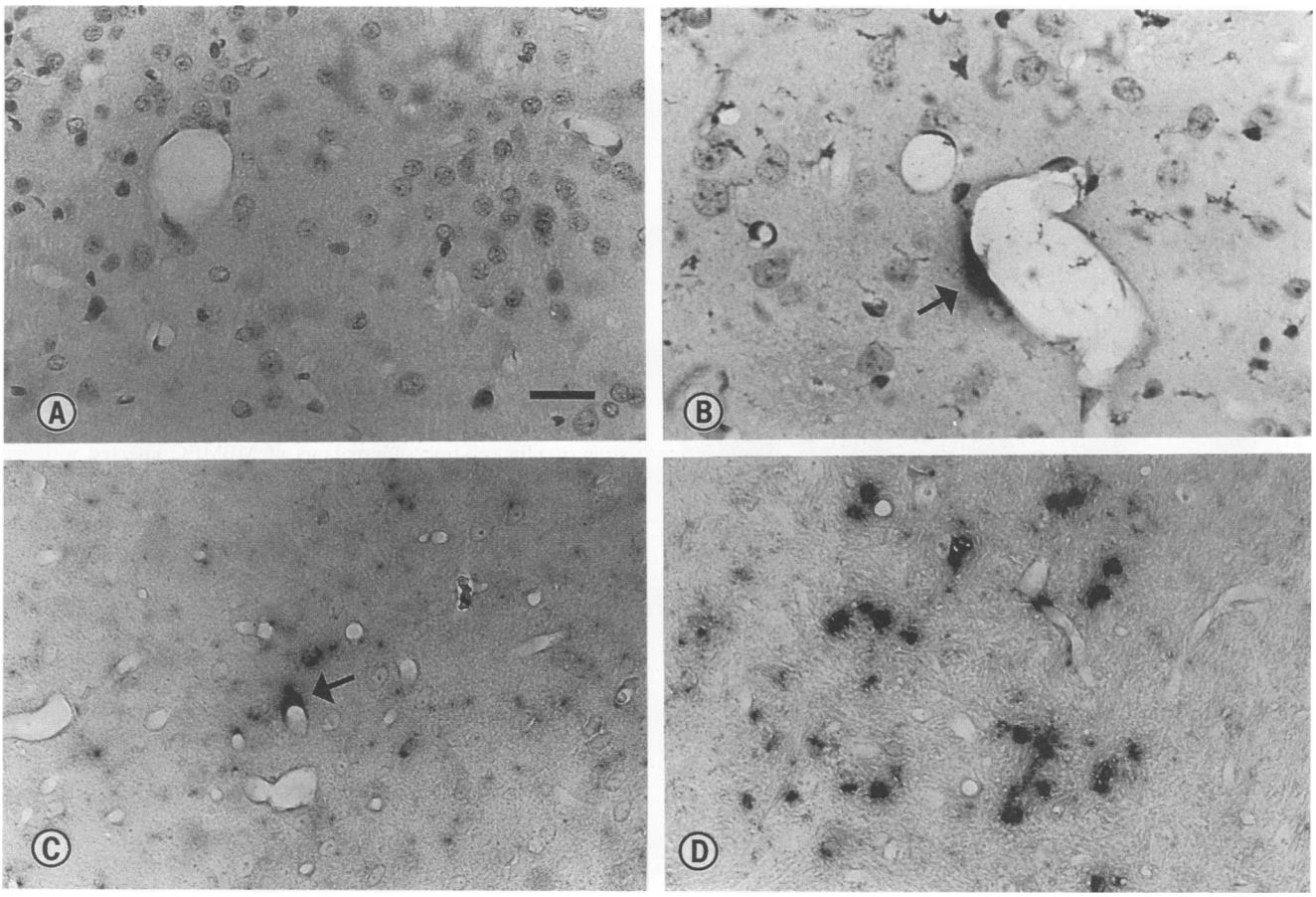

FIG. 3. In situ hybridization of BALB/c mouse CNS sections for SFV-A7 RNA. Panel A represents an uninfected mouse, whereas panels B to D represent mice infected intraperitoneally with 10^6 PFU of SFV-A7 and sacrificed at day 4 p.i. The nonradioactive probe was a 295-nucleotide double-stranded DNA fragment from the E1 area of the SFV-A7 genome, labeled with DIG-11-dUTP by random priming. The capillary EC reactive with the probe are indicated by the arrows in panels B and C. Panel D shows a typical focus of infected cells. All the panels shown are from cerebral hemispheres. The staining was with hematoxylin-eosin (A and B) or eosin only (C and D). Magnification: the scale bar shown in panel A corresponds to 50 μm in panels A, C, and D and 31 μm in panel B.

sels and their intensity of staining increased from day 3 p.i., peaked on days 5 to 6 (Fig. 1D), and thereafter gradually declined to the basal low level. The expression correlated with the mononuclear cell infiltration identified in immunohistochemical staining for T-cell and monocyte cell surface antigens (data not shown). Simultaneously, appearance of viral antigens in CNS on and around blood vessels was observed (Fig. 1A) and was followed by leakage of fibrinogen from the vessels into brain parenchyma (Fig. 1B).

TABLE 1. SFV-A7 RNA in CNS of BALB/c mice in experimental virus infection: an in situ hybridization analysis

Days p.i.	No. of SFV-A7 RNA-positive cells/section[a]	Range	No. of sections studied
0	0	0	32
1	0.3	0.3–0.3	18
2	3.2	1.9–4.4	25
3	5.7	3.7–7.7	24
4	5.8	1.9–9.7	30
5	1.2	0.6–1.8	38
6	1.8	1.3–2.2	34
7	0.3	0.2–0.4	33

[a] The average value of two mice per time point, analyzed in two separate in situ hybridization runs.

Culture and characterization of MBMEC. To study whether the observed induction of ICAM-1 during SFV-A7 infection was directly caused by the virus and whether virus antigen expression on and around vascular EC was associated with cell injury, we set up a system for culturing mouse brain capillary EC in vitro. When EC are prepared from mouse brain, it is essential to verify that the culture is homogeneous for these cells. The reason for this is that the isolation procedure may trap other cell types, such as smooth muscle cells or astrocytes. The marker we used to identify EC was FITC-coupled *Griffonia simplicifolia*, a lectin detecting EC of mouse origin. In addition, the MBMEC were tested for the ability to uptake acetylated LDL (DiI-Ac-LDL), a function mediated by specific receptors typically found on EC. The EC used were from the second or third passage and showed positive staining with GSA-FITC (Fig. 4A), which was inhibited by a preincubation of the lectin conjugate with 0.2 M D(+)-galactose. Fluorescein-activated cell sorter (FACS) analysis indicated that 99% of the cells from the initial passages stained with GSA-FITC, while fewer than 1% were positive after the endothelium-binding carbohydrate

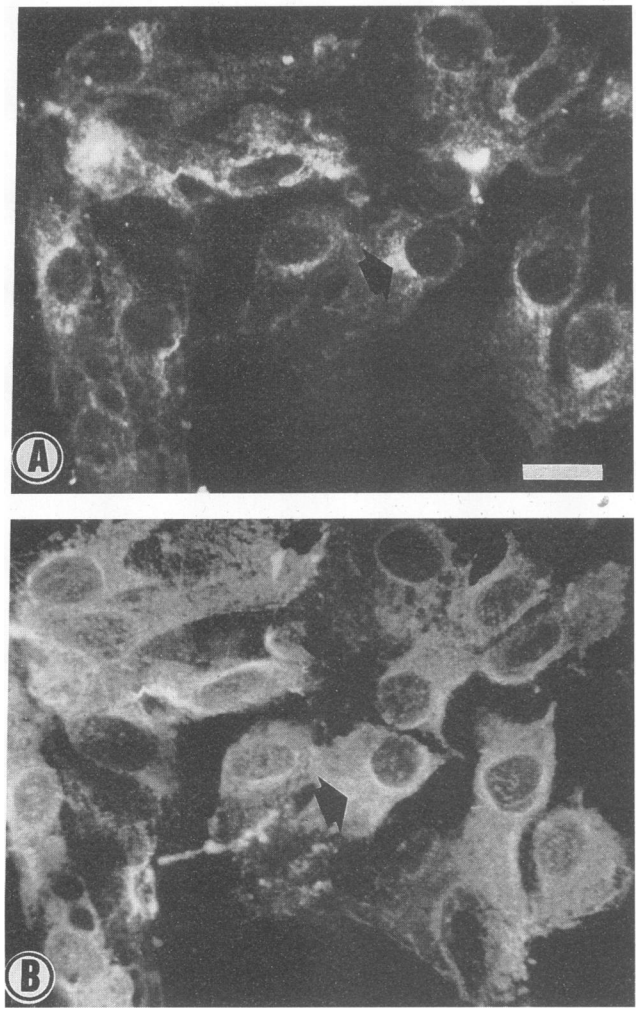

FIG. 4. Detection of SFV-A7 antigens in mouse brain EC in vitro. The cells were infected with SFV-A7 with MOI of 10 and stained for double immunofluorescence 8 h p.i. with an EC marker, GSA-FITC (A), and rabbit antibody to SFV-A7 followed by rhodamine-conjugated goat anti-rabbit IgG (B) as described in Materials and Methods. Arrows in panels A and B indicate an identical cell. Magnification: scale bar = 20 μm.

residues of the lectin conjugate were blocked with 2 mM D(+)-galactose. The MBMEC showed a strong accumulation of DiI-Ac-LDL, unlike MBA-13 cells, a transformed mouse brain cell line, which served as a negative control. Astrocyte contamination was minimal as shown by fewer than 1% of the cells staining positively with rabbit anti-human glial fibrillary acidic protein (data not shown).

Replication of SFV-A7 in MBMEC. To study the replication of SFV-A7 in MBMEC, indirect immunofluorescence staining for virus antigens was first done with specific antiserum. The experiment revealed that by 24 h (after three to four cycles of virus replication) almost all of the cells were infected and that by 72 h all of them were lysed. Double immunofluorescence confirmed the endothelial origin of the infected cells (Fig. 4). The infection was productive, as shown by an increase in virus titer peaking at 11 to 24 h p.i. (Fig. 5).

ICAM-1 expression in vitro. Stimulation of the EC with 200 IU of recombinant murine gamma interferon per ml or 20 IU of recombinant human interleukin-1β per ml for 24 h caused increased expression of ICAM-1, which was expressed at low levels also on unstimulated EC, as studied by indirect immunofluorescence. Infection of the cells with SFV-A7 did not upregulate ICAM-1 after infection with low (0.5 MOI) or high (10 MOI) multiplicity, as studied by immunofluorescence at 4, 6, 12, 24, and 48 h p.i. and by FACS analysis 18 h p.i. (data not shown).

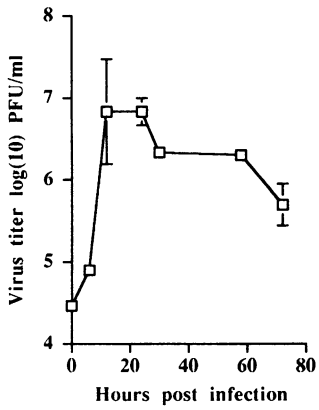

FIG. 5. Growth curve of SFV-A7 in MBMEC. The line indicates virus titer in cell-free supernatants of MBMEC infected with high MOI. The samples were collected at 0, 6, 11, 24, 30, 58, and 72 h p.i. Datum points represent mean ± standard error of the mean values obtained in three separate experiments. Error bars are omitted when smaller than the datum point symbol.

DISCUSSION

We have shown that infection by a nonpathogenic mutant of SFV (SFV-A7) in mice leads to expression of viral nucleic acids and antigens on brain vascular EC and in perivascular neurons. Leakage of fibrinogen occurred at areas with viral antigens. Increased ICAM-1 expression in the brain during SFV infection correlated with the mononuclear cell infiltration. Virus infection of mouse brain EC with the same strain in vitro led to production of infectious virus, but no increase in ICAM-1 expression was observed.

SFV-A7 virus infection in mouse EC in vitro caused lytic infection. Similar EC damage has been described for some other virus infections. Marburg virus, the cause of a fulminating form of hemorrhagic fever, has been shown to replicate in human umbilical vein EC and in organ culture of human umbilical veins to high titers, causing partial EC lysis. It has been suggested that viral damage to the endothelial integrity is a primary pathogenic mechanism in this virus-induced hemorrhagic disease (35). The etiological agent of Korean hemorrhagic fever, Hantaan virus, has also been shown to replicate in human umbilical vein EC but without any obvious cytopathic effect (28).

The EC injury leads to increased fluid permeability (30). We showed increased cerebral vascular leakiness during SFV-A7 infection by detecting fibrinogen in the extravascular space of the brain in areas with virus antigen. As fibrinogen is a serum protein which does not pass intact BBB (31), our results indicate that damage on BBB occurs during SFV infection. Vascular leakiness within the CNS could be caused by virus infection of the EC as viral antigens and nucleic acids were detected in the blood vessel wall in vivo and SFV-A7 replicated in MBMEC in vitro, causing lysis of the cells.

It has been suggested earlier that SFV enters into the brain from the blood by passage across cerebral EC as studied by electron microscopy (27). Recently, in situ hybridization and autoradiographic studies showed SFV-A7 and wild-type virus infection in the CNS as scattered, perivascular foci (13). Our results demonstrating SFV-A7 replication in mouse brain EC in vitro and infection of EC in vivo strongly favor this hypothesis. Viral replication within capillary EC could lead to cytolysis, EC damage, and virus dissemination into the brain parenchyma.

Virus infection of the brain EC may have also other consequences. Vascular leakiness diminishes the shear force provided by flowing blood moving parallel to the EC surface. Diminished shear force favors leukocyte adherence to the EC surface (30). Thus, the direct EC damage caused by SFV-A7 infection of EC could be a mechanism for leukocyte recruitment into the CNS in murine SFV-A7 infection, during which marked infiltrates of immune cells can be seen in histochemical staining of brain and spinal cord tissue although the animals remain asymptomatic (6).

Reduction in shear force acts in concert with concomitant increase in the leukocyte-EC adhesive interactions (30). The molecular basis of increased leukocyte-EC adhesiveness during inflammation has been under extensive investigation during the past few years. It is now apparent that there are inducible adhesion molecules both on leukocyte and on EC surfaces and that the interaction during the adhesion and transmigration process is dynamic, such that the relevant molecules change as the process proceeds (8). Our results indicate that ICAM-1 is induced during SFV-A7 infection following appearance of viral antigens in CNS. However, infection of mouse brain EC by SFV-A7 in vitro did not cause increased cell surface expression of ICAM-1, whereas its expression was induced by gamma interferon and interleukin-1β in accordance with earlier reports (12). We suggest that the induction of ICAM-1 expression during SFV-A7 infection in vivo is caused by cytokines secreted by the infiltrating mononuclear cells. Increased ICAM-1 expression on brain vessels could contribute to increased binding of mononuclear cells, providing a mechanism for recruitment of more inflammatory cells into CNS.

We have initiated these studies on SFV-A7 infection in mouse brain EC because this virus enhances development of EAE in the BALB/c mouse (44). Disease activity in chronic relapsing EAE of guinea pigs has been shown to correlate with BBB damage (20) demonstrated by gadolinium-enhanced nuclear magnetic imaging (20). Similarly, foci of BBB leakage have been shown to be the earliest detectable change in the CNS of patients with MS (22). BBB leakage of plasma proteins has also been demonstrated by immunocytological methods from postmortem samples of recently active MS cases (15). Virus infections have been shown to induce relapse phases of MS (3, 37). BBB damage or increased expression of adhesion molecules caused by the virus infection could be possible mechanisms of the observed association, since vascular permeability changes are a central feature of certain virus infections (10, 29) and induction of vascular endothelial adhesion molecules has been shown during viral encephalitis in humans and in monkeys (34, 38). In this report, we show that SFV-A7 infection causes increased ICAM-1 expression in the brain and increased BBB permeability. This could lead to increased adhesion of leukocytes to brain EC and thus facilitate the entry of inflammatory cells into the brain in mice infected with SFV-A7 after challenge with spinal cord homogenate. This could lead to earlier appearance of EAE signs and symptoms and larger proportion of affected BALB/c mice in EAE with SFV-A7 infection than without viral facilitation. We suggest that facilitation of leukocyte entry to the CNS is a major mechanism for EAE facilitation in the BALB/c mouse by SFV-A7.

In conclusion, an avirulent mutant of a neurotropic SFV, SFV-A7, causes both direct and immune-mediated injury to murine cerebrovascular EC. This could be one mechanism of viral facilitation of EAE. Whether common virus infections are capable of causing hitherto-unrevealed cerebral vascular permeability alterations or inducing adhesion molecules on brain vascular EC in MS patients is a challenging question remaining to be investigated.

ACKNOWLEDGMENTS

This work was supported by the Sigfrid Juselius Foundation.

The SFV-A7 E1 clone was a generous gift from Ari Hinkkanen, University of Turku. We thank Terttu Lauren, Merja Virtanen, and Outi Asunta for excellent technical assistance.

REFERENCES

1. **Ades, E., J. Hierholzer, V. George, J. Black, and F. Candal.** 1992. Viral susceptibility of an immortalized human microvascular endothelial cell line. J. Virol. Methods **39**:83–90.
2. **Allen, I., and B. Branklin.** 1993. Pathogenesis of multiple sclerosis—the immune diathesis and the role of viruses. J. Neuropathol. Exp. Neurol. **52**:95–105.
3. **Anderson, O., P.-E. Lygner, T. Bergström, M. Anderson, and A. Vahlne.** 1993. Viral infections trigger multiple sclerosis relapses: a prospective seroepidemiological study. J. Neurol. **240**:417–422.
4. **Archelos, J. J., S. Jung, M. Mäurer, M. Schmied, H. Lassmann, T. Tamatani, M. Miyasaka, K. Toyka, and H.-P. Hartung.** 1993. Inhibition of experimental allergic encephalomyelitis by an antibody to the intercellular adhesion molecule ICAM-1. Ann. Neurol. **34**:145–154.
5. **Benditt, E., T. Barnett, and J. McCougall.** 1983. Viruses in the etiology of atherosclerosis. Proc. Natl. Acad. Sci. USA **80**:6386–6389.
6. **Berger, M. L.** 1980. Humoral and cell-mediated immune mechanisms in the production of pathology in avirulent Semliki Forest virus encephalitis. Infect. Immun. **30**:244–253.
7. **Bradish, C. J., K. Allner, and H. B. Maber.** 1971. The virulence of original and derived strains of Semliki Forest virus for mice, guinea-pigs and rabbits. J. Gen. Virol. **12**:141–160.
8. **Butcher, E. C.** 1991. Leucocyte-endothelial cell recognition: three (or more) steps to specificity and diversity. Cell **67**:1033–1036.
9. **Cannella, B., A. Cross, and C. Raine.** 1990. Upregulation and coexpression of adhesion molecules correlate with relapsing autoimmune demyelination in the central nervous system. J. Exp. Med. **172**:1521–1524.
10. **Cosgriff, T.** 1989. Viruses and hemostasis. Rev. Infect. Dis. **11**: S672–S688.
11. **DeBault, L., L. Kahn, S. Fromme, and P. Cancilla.** 1979. Cerebral microvessels and derived cells in tissue culture: isolation and preliminary characterization. In Vitro **15**:473–486.
12. **Fabry, Z., M. Waldsmith, D. Hendrickson, J. Keiner, L. Love-Homan, F. Takei, and M. N. Hart.** 1992. Adhesion molecules on murine brain microvascular endothelial cells: expression and regulation of ICAM-1 and Lgp 55. J. Neuroimmunol. **36**:1–11.
13. **Fazakerley, J., S. Pathak, M. Scallan, S. Amor, and H. Dyson.** 1993. Replication of the A7(74) strain of Semliki Forest virus is restricted in neurons. Virology **195**:627–637.
14. **Friedman, H., E. Macarak, R. MacGregor, J. Wolfe, and N. Kefalides.** 1981. Virus infection of endothelial cells. J. Infect. Dis. **142**:266–273.
15. **Gay, D., and M. Esiri.** 1991. Blood-brain barrier damage in acute multiple sclerosis plaques. An immunocytological study. Brain **114**:557–572.
16. **Goldstein, G., A. Betz, and P. Bowman.** 1984. Use of isolated brain capillaries and cultured endothelial cells to study the blood-brain barrier. Fed. Proc. **43**:191–195.
17. **Grossman, R. I., F. Gonzales-Scarano, S. W. Atlas, S. Galetta, and D. H. Silberberg.** 1986. Gadolinium enhancement in MRI imag-

ing. Radiology **161:**721–725.
18. **Haas, J., and E. Yunis.** 1970. Viral crystalline arrays in human coxsackie myocarditis. Lab. Invest. **23:**442–446.
19. **Hänninen, P., P. Arstila, H. Lang, A. Salmi, and M. Panelius.** 1980. Involvement of the central nervous system in acute, uncomplicated measles virus infection. J. Clin. Microbiol. **11:**610–613.
20. **Hawkins, C. P., F. Mackenzie, P. Tofts, E. P. Du Boulay, and W. I. McDonald.** 1991. Patterns of blood-brain barrier breakdown in inflammatory demyelination. Brain **114:**801–810.
21. **Hukkanen, V., P. Heino, A. E. Sears, and B. Roizman.** 1990. Detection of herpes simplex virus latency-associated RNA in mouse trigeminal ganglia by in situ hybridization using nonradioactive digoxigenin-labelled DNA and RNA probes. Methods Mol. Cell. Biol. **2:**70–81.
22. **Kermode, A. G., P. S. Tofts, D. G. MacManus, B. E. Kendall, D. P. E. Kingsley, I. F. Moseley, E. P. G. H. du Boylay, and W. I. McDonald.** 1988. Early lesions in multiple sclerosis. Lancet **ii:** 1203–1204.
23. **Lathey, J., C. Wiley, A. Verity, and J. Nelson.** 1990. Cultured human brain capillary endothelial cells are permissive for infection by human cytomegalovirus. Virology **176:**266–273.
24. **Maples, J. A.** 1985. A method for the covalent attachment of cells to glass slides for use in immunohistochemical assays. Am. J. Clin. Pathol. **83:**356–363.
25. **McCarron, R. M., L. Wang, M. K. Racke, D. E. McFarlin, and M. Spatz.** 1993. Cytokine-regulated adhesion between encephalitogenic T-lymphocytes and cerebrovascular endothelial cells. J. Neuroimmunol. **43:**23–30.
26. **Mokhtarian, F., D. McFarlin, and C. Raine.** 1984. Adoptive transfer of myelin basic protein sensitized T-cells produce chronic relapsing demyelinating disease in mice. Nature (London) **309:** 356–358.
27. **Pathak, S., and H. E. Webb.** 1974. Possible mechanisms for the transport of Semliki Forest virus into and within mouse brain: an electron microscopic study. J. Neurol. Sci. **23:**175–184.
28. **Pensiero, M. N., J. B. Sharefkin, C. W. Dieffenbach, and J. Hay.** 1992. Hantaan virus infection of human endothelial cells. J. Virol. **66:**5929–5936.
29. **Petito, C., and K. Cash.** 1992. Blood-brain barrier abnormalities in acquired immunodeficiency syndrome: immunohistochemical localization of serum proteins in postmortem brain. Ann. Neurol. **32:**658–666.
30. **Pober, J., and R. Cotran.** 1990. The role of endothelial cells in inflammation. Transplantation **50:**537–544.
31. **Reese, T. S., and M. J. Karnovsky.** 1967. Fine structural localization of a blood-brain barrier to exogenous peroxidase. J. Cell Biol. **34:**207–217.
32. **Sahagun, G., S. Moore, Z. Fabry, R. Schelper, and M. N. Hart.** 1989. Purification of murine endothelial cell cultures by flow cytometry using fluorescein-labeled Griffonia Simplicifolia agglutinin. Am. J. Pathol. **134:**1227–1232.
33. **Sandberg, M., and E. Vuorio.** 1987. Localization of types I, II and III collagen mRNAs in developing human skeletal tissues by in situ hybridization. J. Cell Biol. **104:**1077–1084.
34. **Sasseville, V., W. Newman, A. Lackner, M. Smith, N. Lausen, D. Beall, and D. Ringler.** 1992. Elevated vascular cell adhesion molecule-1 in AIDS encephalitis induced by simian immunodeficiency virus. Am. J. Pathol. **141:**1021–1030.
35. **Schnittler, H.-J., F. Mahner, D. Drenckhahn, H.-D. Klenk, and H. Feldmann.** 1993. Replication of Marburg virus in human endothelial cells. A possible mechanism for the development of viral hemorrhagic disease. J. Clin. Invest. **91:**1301–1309.
36. **Sharief, M. K., M. A. Noori, M. Ciardi, A. Cirelli, and E. J. Thompson.** 1993. Increased levels of circulating ICAM-1 in serum and cerebrospinal fluid of patients with active multiple sclerosis. Correlation with TNF-α and blood-brain barrier damage. J. Neuroimmunol. **43:**15–22.
37. **Sibley, W. A., C. R. Bamford, and K. Clark.** 1985. Clinical viral infections and multiple sclerosis. Lancet **ii:**1313–1315.
38. **Sobel, R., M. Mitchell, and G. Fondren.** 1990. Intercellular adhesion molecule-1 (ICAM-1) in cellular immune reactions in the human central nervous system. Am. J. Pathol. **136:**1309–1316.
39. **Springer, T. A.** 1990. Adhesion receptors of the immune system. Nature (London) **346:**425–433.
40. **Voyta, J. C., P. A. Netland, D. P. Via, and B. R. Zetter.** 1984. Specific labelling of endothelial cells using fluorescent acetylated low-density lipoprotein. J. Cell Biol. **99:**81A.
41. **Wangel, A., M. Temonen, M. Brummer-Korvenkontio, and A. Vaheri.** 1992. Anti-endothelial cell antibodies in nephropatia epidemica and other viral diseases. Clin. Exp. Immunol. **90:**13–17.
42. **Ward, J., T. O'Leary, G. Baskin, R. Benveniste, C. Harris, P. Nara, and R. Rhodes.** 1987. Immunohistochemical localization of human and simian immunodeficiency viral antigens in fixed tissue sections. Am. J. Pathol. **127:**199–205.
43. **Wiley, C. A., R. S. Schrier, J. A. Nelson, P. W. Lampert, and M. B. A. Oldstone.** 1986. Cellular localization of human immunodeficiency virus infection within the brains of acquired immune deficiency syndrome patients. Proc. Natl. Acad. Sci. USA **83:**7089–7093.
44. **Wu, L.-X., M. J. Mäkelä, M. Röyttä, and A. Salmi.** 1988. Effect of viral infection on experimental allergic encephalomyelitis in mice. J. Neuroimmunol. **18:**139–153.
45. **Zurbriggen, A., and R. Fujinami.** 1988. Theiler's virus infection in nude mice: viral RNA in vascular endothelial cells. J. Virol. **62:**3589–3596.